Effective Adsorption of Sodium Dodecylsulfate (SDS) by Hydrocalumite (CaAl-LDH-Cl) Induced by Self-dissolution and Re-precipitation Mechanism

Ping Zhang [a,b,c], Guangren Qian [*b], Zhi Ping Xu[d], Huisheng Shi [a], Jing Yang [c], Ray L. Frost [*c]

[a] *School of Environmental and Chemical Engineering, Shanghai University, Shanghai 200072, PR China*

[b] *Key Laboratory of Advanced Civil Engineering Materials (Tongji University), Ministry of Education, Shanghai 200092, PR China*

[c] *Chemistry Discipline, Faculty of Science and Technology, Queensland University of Technology, GPO Box 2434, Brisbane Queensland 4001, Australia*

[d] *Australian Research Council (ARC) Centre of Excellence for Functional Nanomaterials, Australian Institute for Bioengineering and Nanotechnology and School of Engineering, The University of Queensland, Brisbane, QLD 4072, Australia*

Corresponding Authors:

Ray L. Frost: Tel: +61-7-3138 2407;
Fax: +61-7-3138 2407
Email: r.frost@qut.edu.au

Prof. G. Qian: Tel: +86-21-56338094;
Fax: +86-21-56333052.
Email: grqian@shu.edu.cn;

Abstract

Hydrocalumite (CaAl-LDH-Cl) were synthesized through a rehydration method involving a freshly prepared tricalcium aluminate (C_3A) with $CaCl_2$ solution. To understand the intercalation behaviour of sodium dodecylsulfate (SDS) with CaAl-LDH-Cl, X-ray diffraction (XRD), Fourier transform infrared (FTIR), scanning electron microscopy (SEM), transmission electron microscope (TEM), X-ray photoelectron spectroscopy (XPS), inductively coupled plasma-atomic emission spectrometer (ICP) and elemental analysis have been undertaken. The sorption isotherms with SDS reveal that the maximum sorption amount of SDS by CaAl-LDH-Cl could reach 3.67 $mmol \cdot g^{-1}$. The results revealed that CaAl-LDH-Cl holds a self-dissolution property, about 20-30% of which is dissolved. And the dissolved Ca^{2+}, Al^{3+} ions are combined with SDS to form CaAl-SDS or Ca-SDS precipitation. It has been highlighted that the composition of resulting products is strongly dependent upon the SDS concentration. With increasing SDS concentrations, the main resulting product changes from CaAl-SDS to Ca-SDS, and the value of interlayer spacing increased to 3.27 nm.

Keywords: hydrocalumite; sodium dodecylsulfate; mechanism; self-dissolution; precipitation; X-ray photoelectron spectroscopy (XPS).

1. Introduction

Anionic clays, normally named as layered double hydroxides (LDHs) or hydrotalcite-like compounds, can be represented with the general formula $[M^{2+}_{1-x}M^{3+}_{x}(OH)_2]A_{x/n}\cdot yH_2O$, where M^{2+} and M^{3+} are any divalent and trivalent metal cations, A^{n-} is the interlayer anions, and x is $M^{3+}/(M^{2+}+M^{3+})$ molar ratio [1, 2]. There is an interesting group of LDHs named as hydrocalumite $Ca_2Al(OH)_6Cl(H_2O)_2\cdot mH_2O$. A net positive charge on the sheets originates from the partial replacement of Ca^{2+} with Al^{3+} ions, forming $[Ca_2Al(OH)_6^+]$ layers. The distorted "brucite-like" layers were separated by interlayers of water molecules and Cl^- [3]. Hydrocalumite was mainly produced in cements, which was critical in the function and stablity of salt-saturated portland cement-based grouts [4, 5]. Such grouts were needed to seal exploratory excavations in a radioactive waste repository sited in beded salt [6]. So it was easily and cheaply made through the simple hydration reaction of cement paste with Cl-bearing salt solutions.

Since LDHs were composed by positively charged metal hydroxide sheets compensated by anions in the interlayers, they had a remarkable property that a variety of anionic species, especially organic anions, being inserted as guests into the interlayer region [2, 7]. Kanchan [8] used synthetic MgAl-LDH to uptake of arsenite from aqueous solution by ion exchanged process. Qian and co-workers reported that CaAl-LDH-Cl removed selenate or Cr(VI) from aqueous solution by anionic exchange mainly. It was worth paying close attention that these papers referred to the self-dissolved process for CaAl-LDH-Cl and the reprecipitation for CaAl-LDH-Cl and

69 oxyanions [9, 10]. This phenomenon was distinguished from that occurring in
70 MgAl-LDH reaction system.

71 Sodium dodecyl sulfate (SDS) is an anionic surfactant, and widely used in many
72 industrial processes, such as colloid stabilization, metal treatments, mineral flotation,
73 and daily-used detergents and pesticides [11]. SDS and perfluorooctane sulfonate
74 (PFOS) are ascribed as persistence organic pollutants (POPs) [12, 13]. Nowadays
75 the conventional methods for surfactant removal from water involved processes, such
76 as chemical and electrochemical oxidation, membrane technology, chemical
77 precipitation, photo-catalytic degradation, adsorption and various biological methods
78 [14-18]. Many of these processes are not cost effective. Adsorption technology can
79 offer potential low-cost treatment of these pollutants, by using soil, activated carbon
80 and clays, but after adsorbing SDS, their products were difficult to recycle [15, 19].
81 Recently, some researchers used SDS to modify LDHs surface properties, and then to
82 adsorb non-ionic organic compounds from wastewater [6, 20-22]. Zhao [23] reported
83 the syntheses of a series of organic-inorganic nanocomposite of dodecylsulfate-LDHs
84 by MgAl-LDH to trap chlorinated organic pollutants in water. It was understood that
85 SDS sorption occurred on edge/external surfaces. Other reports [24] introduced SDS
86 into ZnAl-LDH to form organo-LDH by an ion-exchange method. So It is perfectly
87 reasonable to use LDH to removal SDS. The by-product was still able to be exploited
88 as valuable resources to dispose of organic matter from wastewater.

89 This study has used XPS to determine both the chemical bonding of Ca and Al
90 from samples collected before and after adsorption SDS onto CaAl-LDH-Cl. X-ray

photoelectron spectroscopy (XPS) has become an increasingly effective tool for investigating the nature of many different types of surfaces, which is an important, established and frequently essential tool for understanding several important aspects of nano-structured natural [25, 26]. In fact, both elemental and chemical state XPS imaging and, in particular, a relatively new method of qualitative or (semi-) quantitative XPS imaging, has been used to investigate the chemical environment of elements from the various LDHs phases within intercalation process [27-29].

Thus, this research focuses on using CaAl-LDH-Cl to adsorb sodium dodecylsulfate from aqueous media. The objectives of this research are: (1) investigate DS adsorption from aqueous solution with CaAl-LDH-Cl; (2) understand the intercalation mechanism of DS over this LDH. It has been found that CaAl-LDH-Cl underwent dissolution, and consequently the XRD results of CaAl-LDH-Cl modified by DS showed two phases. We propose that the intercalation mechanism is more dependent on the precipitation than the so-called anion exchange.

2. Experimental Section

2.1 Materials synthesis

Preparation of CaAl-LDH-Cl materials

The CaAl-LDH-Cl materials were synthesized by hydrating freshly prepared tricalcium aluminate (C_3A) in $CaCl_2$ solution. The solid phase reaction was used to synthesize tricalcium aluminate (C_3A) by heating reagent grade $CaCO_3$ and low-alkali Al_2O_3 in a molar ratio of 3:1 at 300-1350 ^{o}C. The heating process was conducted in a

quartz crucible and continued until the free lime content was reduced to below 0.5%, as evidenced by X-ray powder diffraction and a modified Franke test. Then, the as-prepared solid was mixed with $CaCl_2 \cdot 6H_2O$ solution. During the hydration process, the suspension was continuously shaken for more than 18 h under N_2 at a temperature of 55±1°C. After cooling to room temperature, the suspension was filtered and the obtained cake was extensively washed with double distilled CO_2-free water until the filtrate was free of Cl^- ion ($AgNO_3$ test). The cake was dried at 105 ^{o}C overnight, and then ground and stored in a plastic bottle. According to the elemental analysis of the synthesised sample, the chemical formula is $Ca_{3.9}Al_2(OH)_{11.2}Cl_2(CO_3)_{0.3} \cdot 4.1H_2O$ (M.W.=563.2 g/mol).

Preparation of CaAl-LDH-Cl interacted with different concentrations of SDS

0.1 g CaAl-LDH-Cl was added to different concentrations of SDS aqueous solutions (20 ml) with concentration of 0.005, 0.01, 0.02, 0.04, 0.08, 0.10 and 0.20 M, respectively. The mixture was centrifuged after stirring at 25 ^{o}C for 24 h. The precipitate was dried at 70 ^{o}C for 24 h in an oven, then ground, passed through a 100 mesh sieve, and seven samples were named the products named as [CaAl-SDS_{005}], [CaAl-SDS_{01}] [CaAl-SDS_{02}], [CaAl-SDS_{04}], [CaAl-SDS_{08}], [CaAl-SDS_1] and [CaAl-SDS_2], respectively. Finally, these samples were stored for characterization. In addition, $CaCl_2$ instead of CaAl-LDH-Cl was used to prepare the precipitate (named as [Ca-SDS]), followed by the same post treatment.

To further understand the SDS removal mechanism, after the corresponding mixed suspensions centrifugation described above, concentrations of SDS, Cl, Ca and Al ions in the supernatant were determined. The concentration of DS from aqueous solution were measured in a Liquid Phase Total Organic Carbon analyzer (Multi N/C 2100), and the concentration of DS from solid products were measured by Elemental analyzer (Euro EA3000), Cl ion concentrations were determined with an ion chromatograph (METROSEP A SUPP 5 – 250) at a flow rate of 0.7 $ml \cdot min^{-1}$, and the eluent was 3.2 mM Na_2CO_3 / 1.0 mM $NaHCO_3$. The concentrations of Ca and Al ions in supernatants were measured with Inductively Coupled Plasma-Atomic Emission Spectrometer (Perkin Elimer Optima DV 2000 ICP-AES).

Additionally, the [MgAl-SDS] solid was prepared by simultaneously adding dropwise an aqueous solution of NaOH (1.5 M) and a mixed aqueous solution of $MgCl_2 \cdot 6H_2O$ and $AlCl_3 \cdot 6H_2O$ into a 500 ml flask containing 0.2 M SDS under vigorously stirring at room temperature, then shaken at 60 ^oC for 24 h and aged at 65 ^oC for another 24 h. Afterwards, the suspension solid was filtered and washed for 2 or 3 times using double distilled water, then dried at 70 ^oC for 24 h. Then the dried sample was ground, passed through 100 mesh sieve and stored in a desiccator for further use.

2.2 Characterization

X-ray diffraction. Powder X-ray diffraction (XRD) data were collected at room temperature in a D/max RBX diffractometer with Cu Kα (40 kV, 100 mA) radiation. CaAl-LDH-Cl was scanned at a rate of 6° per minute in the range of 2θ from 5° to 65°.

157 For the samples adsorbed by different concentrations of SDS, the XRD data were
158 collected in two sections: the first section was scanned from 1° to 5° using silts 1/6
159 (divergence), 1/6 (anti-scattering) and 0.15 (receiving) at a rate of 0.5° per minute and
160 the second section from 5° to 65° using silts 1/6 (divergence), 1/6 (anti-scattering) and
161 0.30 (receiving) at a rate of 6° per minute.

162 ***FT-IR***. Fourier transform infrared (FT-IR) spectra were recorded by the Thermo
163 Nicolet AVATAR 370 in the range 4000 – 600 cm^{-1} with 4 cm^{-1} resolution by
164 measuring the absorbance of KBr disk containing 1-2 wt% samples.

165

166 ***XPS.*** Data was acquired using a Kratos Axis ULTRA X-ray photoelectronspectro-
167 meter incorporating a 165 mm hemispherical electron energy analyzer. The incident
168 radiation was monochromatic Al KR X-rays (1486.6 eV) at 150 W (15 kV, 10 mA)
169 and at 45° to the sample surface. Photoelectron data was collected at take off angle of
170 θ) 90°. Survey (wide) scans were taken at an analyzer pass energy of 160 eV and
171 multiplex (narrow) high resolution scans of Ca 2p, Al 2p, O 1s and S 2p at pass
172 energy of 20 eV. Survey scans were carried out over 1200-0 eV binding energy range
173 with 1.0 eV steps and a dwell time of 100 ms. Narrow high-resolution scans were run
174 with 0.05 eV steps and 250 ms dwell time. Base pressure in the analysis chamber was
175 1.0×10^{-9} torr and during sample analysis 1.0×10^{-8} torr. Atomic were calculated
176 using the CaseXPS version 2.3.14 software and a linear baseline with Kratos library
177 Relative Sensitivity Factors (RSFs). A small amount of each finely powdered sample
178 was carefully applied to double-sided adhesive tape on a standard Kratos Axis Ultra

sample bar. This was attached to the sample rod of the Load Lock system for initial evacuation to ~ 1×10^{-6} torr. The sample bar was then transferred to the UHV sample analysis chamber (SAC) for collection of X-ray photo- emission spectra.

SEM. Samples were coated with a thin layer of evaporated gold, and secondary electron images were obtained using a scanning electron microscope，and the electric tension was 30 kV, the working distance was 7mm. (FEI Quanta 200 SEM, FEI Company, Hillsboro, OR).

BET. Surface area analyses based upon N_2 adsorption/desorption techniques were analysed on a Micrometrics Tristar 3000 automated gas adsorption analyser. Before the analysis, samples were pre-treated at 60 °C under the flow of N_2 on a Micrometrics Flowprep 060 degasser. And the selected range of relative pressure is 0.01 to 0.99, the lowest pressure in measurement of the adsorption isotherm is 7.66772 mmHg.

3. Results and discussion

3.1 Adsorption behaviour of SDS in SDS aqueous solution

The sorption isotherm of SDS by CaAl-LDH-Cl in SDS solution was obtained by plotting the amount of adsorbed SDS (Q) versus the solution concentration (C_e) at equilibrium (Fig. 1). As shown in Fig. 1, the adsorbed amount of DS increased steeply from 0.58 to 3.03 mmol/g at a relatively low SDS initial concentration (from 0.005 to 0.04 mol/L). Thereafter, the increase rate slowed down gradually and then reached a sorption equilibrium as SDS initial concentration was 0.1 mol/L. The adsorption isotherm was well-fitted to a Langmuir isotherm adsorption model (R^2 = 0.9588),

revealing that CaAl-LDH-Cl had homogeneous surfaces with monolayer adsorption sites for the SDS. The adsorbed maximum amount of SDS by per unit mass of LDH was 3.67 mmol/g, much higher than that adsorbed by other kinds of LDHs, which were around 1 mmol/g [30, 31]. Supposed that 1g CaAl-LDH-Cl contained 3.55 mmol/g Cl ion which were replaced completely by 3.55 mmol/g DS ion. In fact, the actual adsorption amount of SDS was much higher than the theoretical value. So it was easily indicated that the ion-exchanged reaction did not occur between SDS and CaAl-Cl-LDH.

3.2 Characterization of obtained solids

1. X-ray diffraction.

The X-ray diffraction patterns were overwhelmingly supported for the determination of the structure of layered materials. As stated, as-obtained CaAl-LDH-Cl showed the typical XRD patterns similar to that of hydrocalumite in the 2θ region from 5 to 65° (Fig. 2a). All diffraction peaks in this pattern could be indexed as the pure hexagonal phase recorded on PDF 78-1219 in the database of the International Centre for Diffraction Data [32]. The sharp reflections with high intensity as (002), (004), (006), (110) were indicated relatively well-formed crystalline layered structure consisting of distorted “Brucite-like” layers, with its $d_{(002)}$ being 0.78 nm. It was also implied that high purity crystalline CaAl-LDH-Cl was successful synthesized. According to these diffraction peaks, we calculated the cell parameters a = 0.994 nm, b = 0.573 nm and c = 1.594 nm.

222 Fig. 2 illustrated the XRD patterns of solids retaining different concentration of
223 SDS such as [CaAl-SDS_{005}], [CaAl-SDS_{01}], [CaAl-SDS_{02}], [CaAl-SDS_{04}],
224 [CaAl-SDS_{08}], [CaAl-SDS_1] and [CaAl-SDS_2]. With the increase of the surfactant
225 concentration, two different series of reflections are observed (marked with "*" and
226 "#" in Fig.2b), reflecting two types of frameworks contained in the obtained
227 materials.

228 In the 2θ region from 2 to 65°, the samples obtained under 0.02 mol/L SDS
229 concentration ([DS] = 4 mmol/g) displayed reflections with high intensity as (002),
230 (004) and (006), similar to the structure of CaAl-LDH-Cl, illustrating that they kept
231 the $[Ca_2Al(OH)_6]^+$ main layer. Moreover, the (002) reflections of CaAl-LDH-Cl
232 became broader, accompanying the corresponding (004) and (010) reflections jointing
233 to one broad reflection (Fig.2a), indicating that SDS reduces the crystalline form of
234 LDH. Additionally, the reflections at low angles appeared gradually with the
235 reflection represented the distance of LDH's interlayer space shifting to lower angle
236 from 3.42 ^{o} to 3.20 ^{o} (Fig.2b), indicating SDS anions enter the interlayer spaces and
237 the intercalated amount accumulated gradually.

238 As SDS concentration arrived to 0.04 mol/L, another new diffraction pattern
239 began to be observed at lower 2θ angle (<3°). And its intensity became sharper
240 gradually resulted from SDS concentration growing (marked with "*" shown in
241 Fig.2b), and the intensity of diffraction peak marked with "#" decreased in intensity.
242 Taking [CaAl-SDS_2] for example, there were two peaks at 2.74^o and 3.2^o (2θ), and
243 the former was so high in intensity that the latter nearly disappeared. It was suggested

that another layered material was formed when SDS content was higher than 4 mmol/g, and its proportion in the mix crystal had a growing process with SDS content increasing. In terms of Bragg's Law, it was easily calculated that *d* values of two layered materials were 3.25 and 2.72 nm, respectively.

2. Infrared spectroscopy (FTIR)

The FTIR spectra of SDS modified CaAl-LDH-Cl with different concentrations were presented in Fig. 3. In case of CaAl-LDH-Cl with SDS, typical bands of SDS all were observed at corresponding wavenumbers, such as C-H stretching and bending bands (2853-2965 cm^{-1} and 1409 cm^{-1}), $-OSO_3^-$ stretching and bending bands (1229, 1065 and 720 cm^{-1}). The stretching vibrations of lattice water and -OH groups were appeared at 3480 and 3636 cm^{-1} as the strong overlapping bands. The peak at 1621 cm^{-1} was due to the H-O-H bending vibration of the interlayer water molecule. The stretching and deformation vibrations of M-OH were reflected by peaks at 785 cm^{-1} and at 532 cm^{-1} (not shown). It was worthwhile to mention that the details of IR results still had evident differences less than or more than 0.02 mol/L SDS concentration, such as the IR bands at around 790 cm^{-1} and 1220 cm^{-1}, respectively. In case of the solids with low concentration of SDS, the intensity of bands at 790 cm^{-1} were obvious, similar to that of CaAl-LDH-Cl, indicating that the product kept the structure of $[Ca_2Al(OH)_6]^+$ main layer, which was perfect identified with the XRD results. In addition, the $-OSO_3^-$ stretching vibration revealed a intact peak at 1220 cm^{-1}. However, the bands at corresponding position were changed with the SDS

concentration exceeding 0.04 mol/L. The intensity of band at 790 cm^{-1} decreased and dissappeared as the SDS concentration reached 0.2 mol/L, and the $-OSO_3^-$ stretching vibration were separated two peaks with higher intensity clearly at 1248 cm^{-1} and 1216 cm^{-1}. The observation proved that the combined environments of SDS occurred change and the new material was formed without $[Ca_2Al(OH)_6]^+$ main layer at SDS high content. In addition, the -OH related bands shifted to lower wavenumber with SDS content increasing. It is presumed that SDS anions modified CaAl-LDH-Cl could change the surface property from hydrophilicity to hydrophobicity [20].

2. ***X-ray photoelectron spectroscopy (XPS)***

XPS is a proven reliable method for intensive investigation for the oxidation state of atoms in the top few layers of material surfaces with partially filled valence bonds. In this research, some complementary XPS experiments (Al and Ca elements) were checked in order to identify the changed chemical environment before and after modification of CaAl-LDH-Cl by SDS as shown in Fig. 4a (in case of [CaAl-SDS_2] material). It was observed from Fig.4a that the binding energy of Al 2p for CaAl-LDH-Cl was 74.1 eV, and the binding energy of Al 2p for [CaAl-SDS_2] material was 74.5 eV, which obviously shifted to higher binding energy 0.4 eV. However, compared with the binding energy of Al 2p for MgAl-LDH (75.0 eV) referred with reports [33, 34], the observed value for MgAl-SDS (74.9 eV) shifted lower binding energy, decreasing with 0.1 eV. This change was completely different from that of CaAl-LDH-Cl and CaAl-SDS_2, indicated the chemical environment for

Al 2p from CaAl-LDH-Cl to CaAl-SDS was different from that change from MgAl-LDH to MgAl-SDS, as is discussed shortly.

On the other hand, compared with the binding energy of Ca 2p from CaAl-LDH-Cl, CaAl-SDS_2 and Ca-SDS (Fig. 4b), two peaks were required to curve fit the Ca $2p_{1/2}$ (351.5 and 350.8 eV) and Ca $2p_{3/2}$ (347.9 and 347.2 eV) XPS broadband for [CaAl-SDS_2], which were similar to those of CaAl-LDH-Cl and Ca-SDS, respectively. As addressed shortly, the Ca^{2+} chemical environment in CaAl-SDS_2 was merged with that of Ca-SDS and CaAl-SDS materials, further illustrating SDS reacted with CaAl-LDH-Cl to form two different precipitations, respectively, as discussed shortly.

4. Scan Electron Microscopy (SEM)

The CaAl-LDH-Cl synthesized with SDS different contents displayed different morphologies (Fig. 5). The SEM image revealed that the approximately hexagonal plate-like crystallites of CaAl-Cl-LDH with sharp particle edges and similar particle sizes, with the thickness around few hundred nanometres and the lateral dimension around 2-3 μm (Fig. 5a), which was common in the LDHs [35]. When CaAl-Cl-LDH was added into SDS aqueous solution, the platelets edges appeared cracked and uneven in appearance. The platelets aggregated and became small particles. However, there were still regularity of plate-like particles in the samples synthesized under SDS concentration lower than 0.02 mol/L. It indicated that CaAl-SDS product was still retained similar morphology as CaAl-LDH-Cl. In the case of [CaAl-SDS_2], the

particles kept the layered structure. Their edge was not as sharp as that of CaAl-LDH-Cl, with the size changed to ten nanometres. In addition, the BET results of CaAl-LDH-Cl and CaAl-SDS_2 were found to decrease from 6.26 m^2/g to 1.70 m^2/g, which was in coordinated with other reports referred to MgAl-LDH modified with SDS [36].

3.3 Interaction mechanism

It is well known that chloride LDHs, such as MgAl-LDH and ZnAl-LDH can spontaneously interacted with SDS through an anion exchange [35, 37, 38], because SDS has a higher affinity than chloride for LDH materials:

$$Mg_2Al\text{-}Cl\text{-}LDH + DS^- \rightarrow Mg_2Al\text{-}DS\text{-}LDH + Cl^- \qquad (1)$$

This was also observed in our experiments. As marked in Fig. 7, MgAl-SDS-LDH exhibited a new series of diffraction peaks, with a *d*-spacing of 2.64 nm. However, when CaAl-LDH-Cl was used as an adsorbent to remove DS, the mechanism seems not only to be dependent upon the anion exchange. Theoretically, CaAl-LDH-Cl ($Ca_{3.9}Al_2(OH)_{11.2}Cl_2(CO_3)_{0.3}\cdot 4.1H_2O$) contains 3.55 mmol/g Cl^- amount, if only the anion exchange was considered, the intercalated DS amount was around 3.55 mmol/g, and the ratio of Ca, Al and DS was close to 2:1:1. In fact, the elemental analysis of the collected solid CaAl-SDS_2 revealed that the molecular formula was approximately $Ca_{4.1}Al_{1.9}(OH)_{11.7}(DS)_{2.2}\cdot 2H_2O$. It is obviously shown that Al content was less than DS content and Ca content was more two times than Al content, So it is understood that the Ca ion was not only combined with Al , but also with SDS.

From the XRD pattern of the precipitate resulting from $CaCl_2$ and SDS mixed solution, as shown in Fig. 7, as Ca-SDS. Obviously, Ca-SDS had the XRD pattern similar to that of CaAl-SDS_2, i.e., they had a similar layered structure, with the *d*-spacing (3.27 nm) being identical, except for the broad peaks as marked in Fig. 7 According with the elemental analysis for the as-formed Ca-SDS, it had a molecular formula close to $Ca_{1.95}(DS)_{3.5}(Cl)_{0.3}$, i.e., each Ca^{2+} approximately combined two DS. Furthermore, the FT-IR spectra of CaAl-SDS_2 and Ca-SDS showed similar characteristic vibrations of DS (Fig.8). In particular, the characteristic stretching vibration of S=O/S-O bonds in DS at 1220 cm^{-1} further revealed the difference between the intercalated and precipitated DS. In the case of MgAl-SDS-LDH, there is one broad band at 1220 cm^{-1} (Fig. 8). corresponding to the stretching vibration of–OSO_3 group with C_{3v} symmetry. However, in the case of Ca-SDS, such a band was split into two peaks, indicating the symmetry lowering of sulfate group. The symmetry lowering revealed that three oxygens in sulfate had different interactions with the environment, which could be attributed to the formation of Ca and SDS precipitation.

Furthermore, the chemical environment change of Al 2p before and after CaAl-LDH-Cl modified by SDS were different from that of MgAl-LDH, illustrated the interaction between CaAl-LDH-Cl and SDS was not similar to the mechanism for MgAl-LDH and SDS. Combined with the results of Ca 2p from CaAl-LDH-Cl, CaAl-SDS and Ca-SDS were formed when CaAl-Cl-LDH was added into SDS aqueous solution.

353 To understand clearly the intercalated mechanism for CaAl-LDH-Cl and SDS, We
354 investigated the concentrations of Ca, Al, and Cl ion during CaAl-LDH-Cl was
355 interacted with different concentrations of SDS aqueous solution. From Fig. 9, we
356 found that when 5.00 g/L CaAl-LDH-Cl was added into pure water, there were 2.24
357 $mmol \cdot g^{-1}$ Ca ion, 1.15 $mmol \cdot g^{-1}$Al ion and 1.14 $mmol \cdot g^{-1}$ Cl ion in this solution,
358 respectively. The ratio of dissolved Ca, Al and Cl ion was close to 2:1:1, similar to
359 that in CaAl-LDH-Cl, with the final pH 11.41. In terms of this pH value, it is regarded
360 Al ion as $Al(OH)_4^-$ form existing in this solution. So we suggested that the dissolution
361 of CaAl-LDH-Cl occurred in water, as follows:

362 $$Ca_4Al_2(OH)_{12}Cl_2(H_2O)_4 \cdot xH_2O \rightarrow 4Ca^{2+} + 2Al(OH)_4^- + 4OH^- + 2Cl^- + (x+4)H_2O \quad (2)$$

363 However, when SDS added into aqueous solution, Ca and Al ion content dropped
364 quickly in solution. Before SDS concentration was less than 0.02 mol/L, the ratio of
365 descent rate of Ca and Al was close to 2, suggested that the precipitated product
366 contained $[Ca_2Al(OH)_6]^+$ main layer. In fact, the changes in XRD and FTIR of
367 [CaAl-SDS_{005}], [CaAl-SDS_{01}] and [CaAl-SDS_{02}] were well proved this deduction. In
368 comparison, the decreased ratio $[Ca^{2+}]/[Al^{3+}]$ was far away from 2 after SDS
369 concentration more than 0.02 mol/L, and uptake amount of SDS continued to increase.
370 As SDS concentration got to 0.2 mol/L, containing 40 mmol/g SDS content, which
371 was ten times more than Cl ion theoretical content in CaAl-Cl-LDH. After the
372 reaction reached equilibrium, there still were 0.7 mmol/g $Al(OH)_4^-$, yet only 0.02
373 $mmol \cdot g^{-1}$ Ca^{2+} remained in solution, and 3.55 $mmol \cdot g^{-1}$ Cl^- was all dissolved into
374 solution, indicated CaAl-LDH-Cl was all dissolved and Ca ion dissolution was

prohibited much more than Al ion to form Ca-SDS precipitation. Indeed, Ca was easier to combine with SDS resulting from the capacity of dehydration [39]. In this situation, the $[Ca^{2+}][SDS]^{2}$ during the reaction process was about 3.5×10^{-5}, much larger than the solubility product of Ca-SDS (Ksp $=3.7\times10^{-10}$) [40], which further demonstrated that the formation of Ca-SDS was occurred under higher concentration.

Based on the results discussed above, both modes of simple anion exchange and self-dissolution followed by re-precipitation were coexist in the adsorption process, yet the self-dissolution followed by re-precipitation was main mechanism in this research. So we can now draw general schemes for the interaction of SDS with CaAl-LDH-Cl in Fig. 9, and this interaction strongly depends on SDS content. When SDS content was below 3.5 mmol/g, CaAl-LDH-Cl occurred self-dissolution and then the dissolved Ca^{2+} combined with $Al(OH)_4^-$ and DS^- to precipitate and formed CaAl-SDS. When SDS content was much more than 3.5 mmol/g, the dissolved Ca^{2+} preferred to choose DS to form Ca-SDS, then combined with part of $Al(OH)_4^-$ ion.

4. Conclusions

From the present study, the CaAl-LDH-Cl was effectively used for the removal of the SDS from aqueous solutions, and the SDS maximum adsorbed amount could get to 3.67 $mmol\cdot g^{-1}$. When SDS effeciently modified CaAl-LDH-Cl, the interlayer distance of resulting solid was expanded to 3.27 nm, and the particle morphology form regular hexagons with irregular platelets. The current research also revealed that the reaction between CaAl-LDH-Cl and SDS was resulted from the self-dissolution of

CaAl-LDH-Cl and precipitation for SDS with the dissolved Ca^{2+} and Al^{3+} ion. In case of SDS content under 3.5 mmol/g (Cl ion theoretical content in CaAl-Cl-LDH), SDS preferred to combine with the dissolved Ca^{2+} and $Al(OH)_4^-$ ion to form [CaAl-SDS] material. As SDS concentration was up from 3.5 mmol/g, the main resulting product was [Ca-SDS] material.

Acknowledgments

The authors gratefully acknowledge infra-structure and morphology checking support of the Queensland University of Technology, Chemistry Discipline, Faculty of Science and Technology. This project is financially supported by National Nature Science Foundation of China No 20907029 and No. 20677037, Shanghai Leading Academic Discipline Project No. S30109.

References

[1] L. Moyo, N. Nhlapo, W. Focke, Journal of Materials Science 43 (2008) 6144.

[2] J. Pisson, C. Taviot-Gueho, Y. Israeli, F. Leroux, P. Munsch, J. Itie, V. Briois, N. Morel-Desrosiers, J. Besses, J. Phys. Chem. B 107 (2003) 9243.

[3] J. Plank, Z. Dai, N. Zouaoui, Journal of Physics and Chemistry of Solids 69 1048.

[4] G. Qian, Y. Cao, P. Chui, J. Tay, Journal of Hazardous Materials 129 (2006) 274.

[5] G. Qian, X. Yang, S. Dong, J. Zhou, Y. Sun, Y. Xu, Q. Liu, Journal of Hazardous Materials 165 (2009) 955.

[6] Z. Xiong, Y. Xu, Chem. Mater 19 (2007) 1452.

[7] M. Herrero, F.M. Labajos, V. Rives, Applied Clay Science 42 (2009) 510.

[8] K. Grover, S. Komarneni, H. Katsuki, Water Research 43 (2009) 3884.

[9] Y. Wu, Y. Chi, H. Bai, G. Qian, Y. Cao, J. Zhou, Y. Xu, Q. Liu, Z.P. Xu, S. Qiao, Journal of Hazardous Materials 176 (2010) 193.

[10] Y. Dai, G. Qian, Y. Cao, Y. Chi, Y. Xu, J. Zhou, Q. Liu, Z.P. Xu, S. Qiao, Journal of Hazardous Materials 170 (2009) 1086.

[11] P.C. Pavan, E.L. Crepaldi, J.B. Valim, Journal of colloid and interface science 229 (2000) 346.

[12] H. Moriwaki, Y. Takagi, M. Tanaka, K. Tsuruho, K. Okitsu, Y. Maeda, Environmental Science & Technology 39 (2005) 3388.

[13] N. Schouten, L.G.J. van der Ham, G.-J.W. Euverink, A.B. de Haan, Water Research 41 (2007) 4233.

[14] L.-H. Tran, P. Drogui, G. Mercier, J.-F. Blais, Journal of Hazardous Materials 170 (2009) 1218.

[15] I. Kowalska, Desalination 221 (2008) 351.

[16] C.L. Hui, X.G. Li, I.M. Hsing, Electrochimica Acta 51 (2005) 711.

[17] S. Chen, M.B. Timmons, J.J. Bisogni Jr, D.J. Aneshansley, Aquacultural Engineering 13 (1994) 163.

[18] M. Anbia, S. Amirmahmoodi, Scientia Iranica In Press, Corrected Proof.

[19] J. Beltrán-Heredia, J. Sánchez-Martín, G. Frutos-Blanco, Separation and Purification Technology 67 (2009) 295.

[20] H. Zhao, K. Nagy, Journal of colloid and interface science 274 (2004) 613.

[21] Z. Shi, M. Sigman, M. Ghosh, R. Dabestani, Environ. Sci. Technol 31 (1997) 3581.

[22] A. Legrouri, M. Lakraimi, A. Barroug, A. De Roy, J. Besse, Water Research 39 (2005) 3441.

[23] S. Prasanna, R. Rao, P. Kamath, Journal of colloid and interface science 304 (2006) 292.

[24] M.Z.B. Hussein, Z. Zainal, C.Y. Ming, Journal of Materials Science Letters 19 (2000) 879.

[25] K.A.D.d.F. Castro, A. Bail, P.B. Groszewicz, G.S. Machado, W.H. Schreiner, F. Wypych, S. Nakagaki, Applied Catalysis A: General 386 (2010) 51.

[26] S. Casenave, H. Martinez, C. Guimon, A. Auroux, V. Hulea, A. Cordoneanu, E. Dumitriu, Thermochimica Acta 379 (2001) 85.

[27] V. Rives, M.a. Angeles Ulibarri, Coordination Chemistry Reviews 181 (1999) 61.
[28] J. Zhou, Z.P. Xu, S. Qiao, Q. Liu, Y. Xu, G. Qian, Journal of Hazardous Materials 189 (2011) 586.
[29] Y. Xu, H. Zhang, X. Duan, Y. Ding, Materials Chemistry and Physics 114 (2009) 795.
[30] P.C. Pavan, E.L. Crepaldi, G. de A. Gomes, J.B. Valim, Colloids and Surfaces A: Physicochemical and Engineering Aspects 154 (1999) 399.
[31] K. Esumi, S. Yamamoto, Colloids and Surfaces A: Physicochemical and Engineering Aspects 137 (1998) 385.
[32] P. Zhang, H. Shi, R. Xiuxiu, Q. Guangren, R. Frost, J. Therm. Anal. Calorim. (2010) 1.
[33] E. Kanezaki, Journal of Materials Science Letters 17 (1998) 371.
[34] H. Zhang, R. Qi, D.G. Evans, X. Duan, Journal of Solid State Chemistry 177 (2004) 772.
[35] K. Okamoto, N. Iyi, T. Sasaki, Applied Clay Science 37 (2007) 23.
[36] F.R. Costa, A. Leuteritz, U. Wagenknecht, D. Jehnichen, L. Häußler, G. Heinrich, Applied Clay Science 38 (2008) 153.
[37] C. Liu, W. Hou, L. Li, Y. Li, S. Liu, Journal of Solid State Chemistry 181 (2008) 1792.
[38] J. Inacio, C. Taviot-Gueho, C. Forano, J. Besse, Applied Clay Science 18 (2001) 255.
[39] L. Zhong, T. Jiao, M. Liu, J. Phys. Chem. B 113 (2009) 8867.
[40] M.d.C. Hernández-Soriano, F. Degryse, E. Smolders, Environmental Pollution In Press, Corrected Proof.

List of Figures

Figure.1 Adsorption isotherms for SDS by CaAl-LDH in SDS aqueous solutions

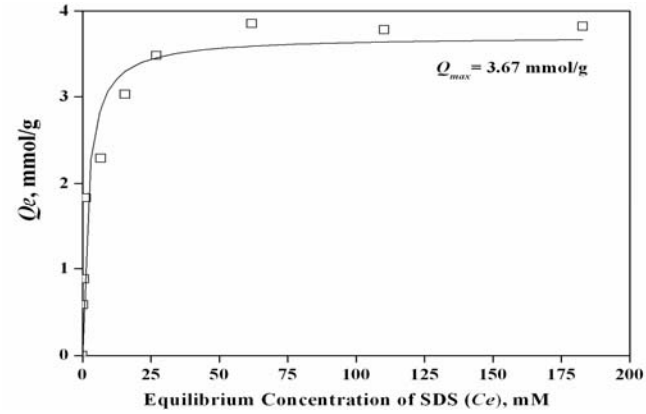

522 Figure.2 The XRD patterns of original CaAl-LDH-Cl, CaAl-SDS_{005}, CaAl-SDS_{01},

523 CaAl-SDS_{04}, CaAl-SDS_{08}, CaAl-SDS_1 and CaAl-SDS_2 scanned from 5°-65° (a) and

524 2.5°-15° (b).

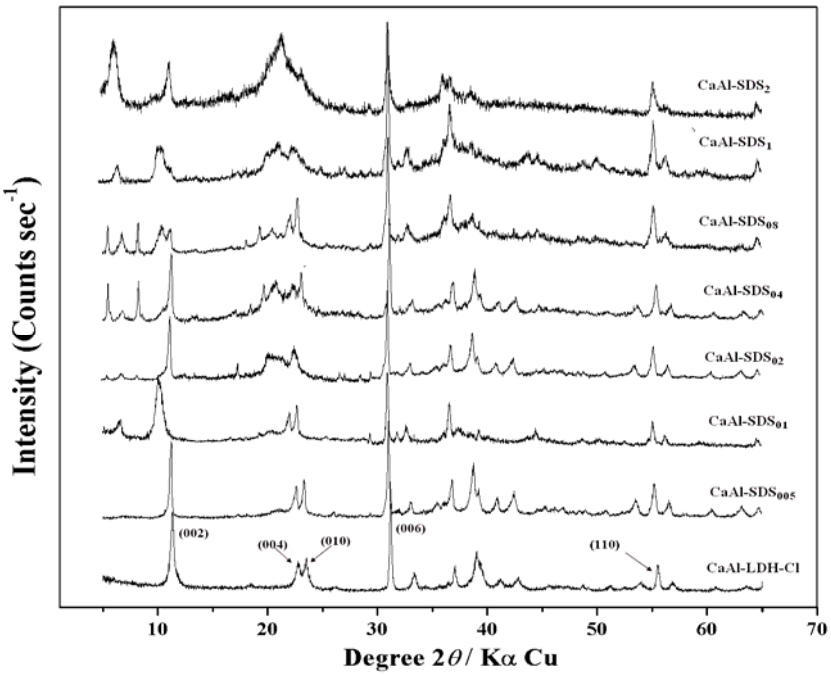

525

526 (a)

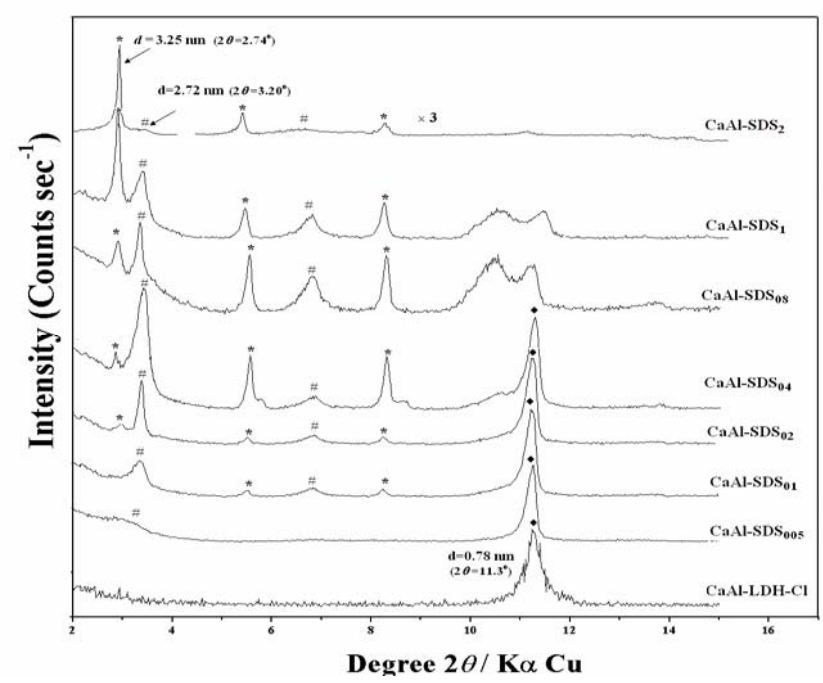

527

528

529 (b)

530

Figure.3 The FT-IR spectra of original CaAl-LDH-Cl, CaAl-SDS$_{005}$, CaAl-SDS$_{01}$, CaAl-SDS$_{04}$, CaAl-SDS$_{08}$, CaAl-SDS$_{1}$ and CaAl-SDS$_{2}$ range from 4000 - 600 cm^{-1}.

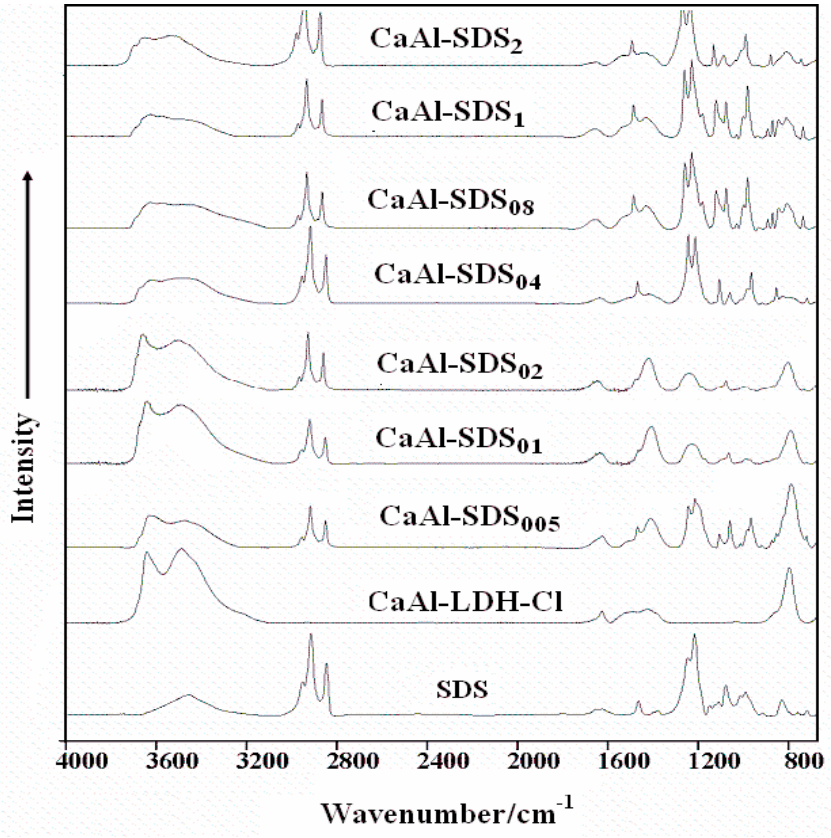

Figure.4 The XPS spectra of Al 2p (a) and Ca 2p (b) from CaAl-LDH-Cl, CaAl-SDS$_2$, Ca-SDS and MgAl-SDS materials.

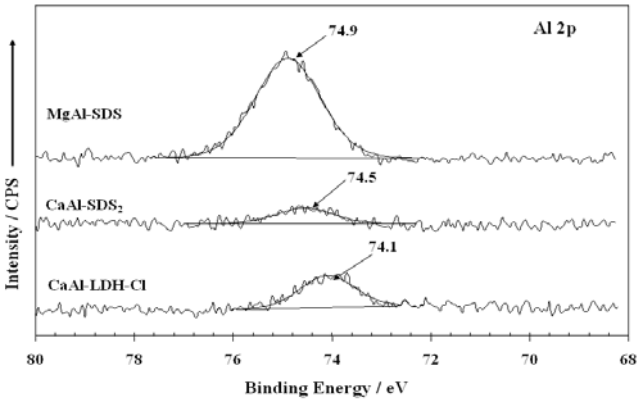

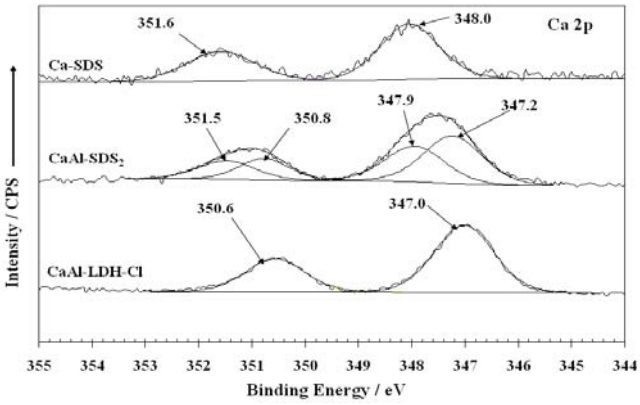

(a)

(b)

Figure.5 The SEM images of (a) CaAl-LDH-Cl; (b) CaAl-SDS$_{005}$; (c) CaAl-SDS$_{04}$; (d) CaAl-SDS$_{08}$; (e) CaAl-SDS$_{1}$ and (f) CaAl-SDS$_{2}$.

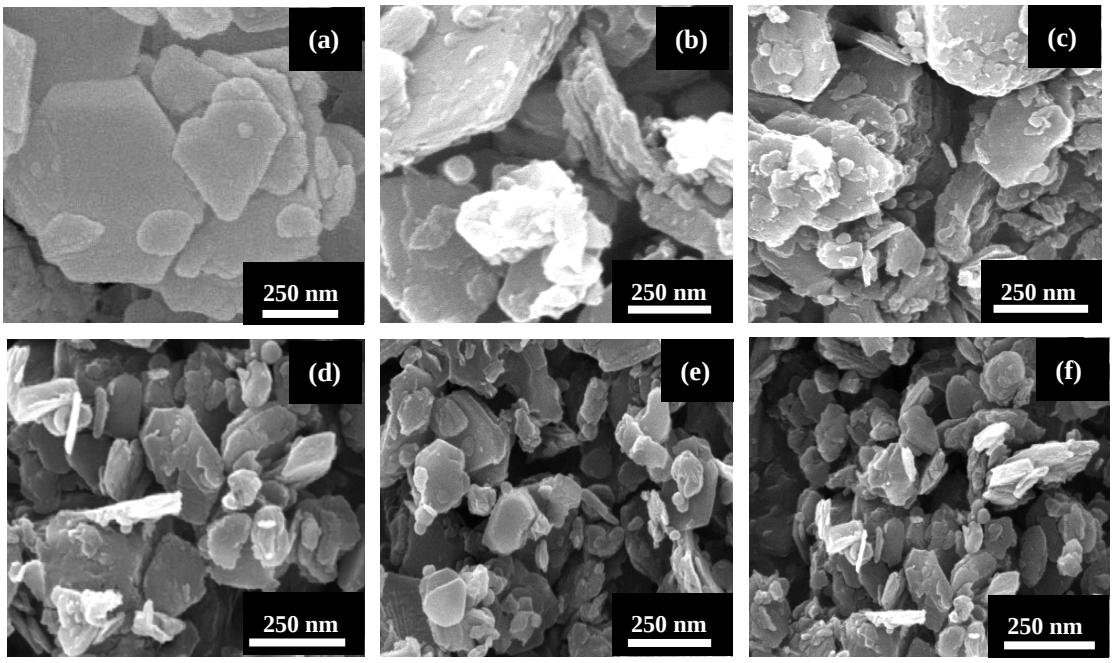

Figure.6 The XRD patterns of the phases obtained from the SDS adsorbed by $CaCl_2$ in 0.2 M SDS aqueous solution and MgAl-LDH in 0.2 M SDS aqueous solution scanned from 1°-15° (The diffraction peaks marked with '*' are attributed to Ca-SDS; those with '#' to Ca/MgAl-SDS.)

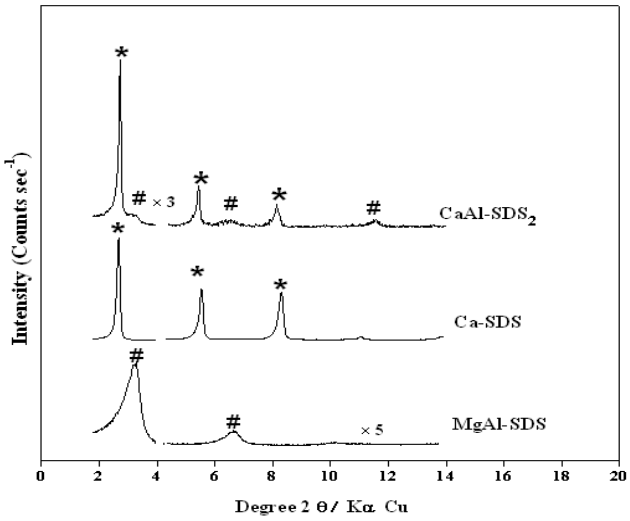

Figure.7 FT-IR spectrum of the phases obtained from the SDS adsorbed by $CaCl_2$ or MgAl-LDH in 0.2 mol·L^{-1} SDS aqueous solution

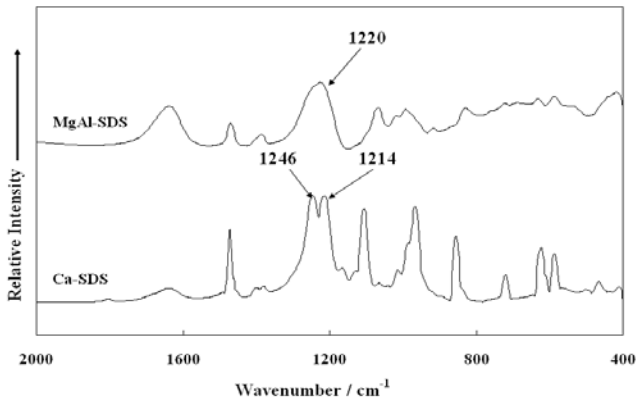

Figure.8 The dissolved amounts of Ca^{2+}, Al^{3+} and Cl^{-} ion during adsorption process in SDS aqueous solutions, respectively.

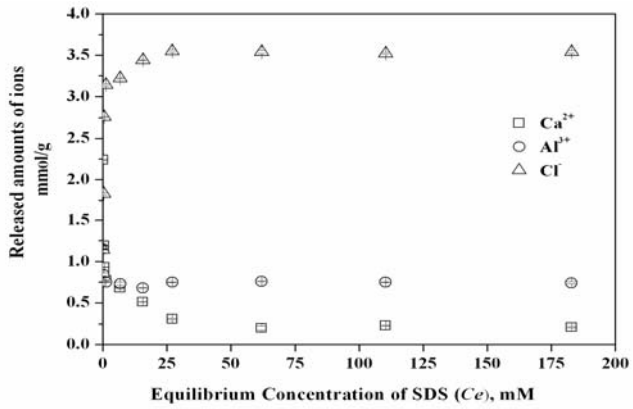

Figure.9 Schematic illustration for the interaction mechanism of CaAl-LDH with SDS. (Ca^{2+} marked with ; $Al(OH)_4^-$ marked with ; SDS marked with .

1) SDS content < 3.55 mmol/g

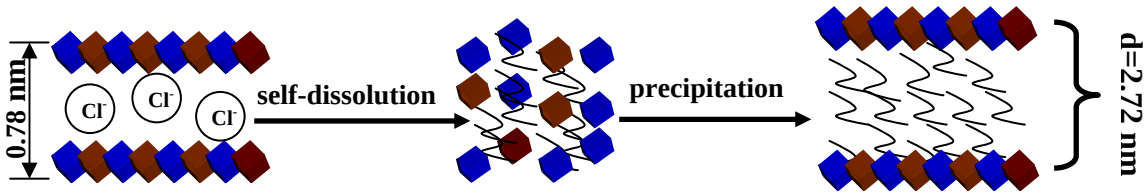

2) 2) SDS content >> 3.55 mmol/g